NANOSCALE PERFORATION OF GRAPHENE BY GRAZING INCIDENCE SWIFT HEAVY ION IRRADIATION

Pavo Dubček[1,*], Damjan Iveković[1], Tihana Čižmar[1], Marko Karlušić[1,*]

1 Ruđer Bošković Institute, Bijenička 54, 10000 Zagreb, Croatia

*Corresponding authors: pavo.dubcek@irb.hr, marko.karlusic@irb.hr

ABSTRACT

In this study, we used atomic force microscopy and Raman spectroscopy to study response of the CVD-grown graphene on SiO_2 substrate to swift heavy ion irradiation at grazing incidence. Irradiation parameters (in terms of ion type, energy, fluence and angle of irradiation) needed for perforation of graphene have been identified, and 4.8 keV/nm electronic stopping threshold has been established. Raman spectroscopy indicates that the production of vacancies is a prerequisite for the perforation of graphene. However, large density of defects introduced by pre-irradiation can hinder the perforation of graphene.

Keywords: swift heavy ion, ion irradiation, Raman spectroscopy, atomic force microscopy, graphene

I. INTRODUCTION

Extraordinary properties of graphene make it an attractive material for the most diverse applications such as nanoelectronics, energy storage, sensors and bio-applications [1]. Various methods of graphene growth yield material of various quality, but it is generally considered that CVD-grown graphene is of excellent quality. This process can be used to produce graphene on a large scale, which can be used for applications where low defect density is required, such as in the production of nanomembranes [2]. In this case, ion irradiation has been shown to be an optimal way to produce nanopores in graphene sheets that act as a filtration element [3,4]. These nanopores have a very narrow size distribution that can be tuned by the ion energy [5,6], while nanopore

density can be set precisely by the applied ion fluence. The mechanical stability of the nanomembrane can be enhanced by choosing suitable support (such as thin polymer film [4]), or by using thicker bilayer and trilayer graphene [7]. Therefore, graphene nanomembranes remain very attractive research topic to this day, as various applications can be targeted by choosing suitable nanopore sizes, while the atomic-scale thickness of graphene should provide unsurpassed permeation rates.

Compared to low energy (keV) ion irradiation, swift heavy ion (SHI) irradiation offers some additional benefits such as long range of ions within the material and large density of deposited energy via electronic stopping, while almost negligible nuclear stopping power results in the absence of collisional cascades. Thus, interactions of this type of energetic ions (MeV energy range and beyond) with graphene can be exploited by suitable choice of irradiation parameters. Of particular interest is the irradiation angle, when grazing incidence SHI irradiation of graphene yields large nanopores, accompanied by folded graphene at their edges [8,9]. The driving force for perforation of graphene and the creation of large nanostructures due to the ion impacts is a very large amount of deposited energy, when there is an extended overlap between the SHI trajectory and graphene, although the exact amount of energy retained within graphene remains an open question [10,11]. Clearly, such drastic irradiation effects have a significant consequence for radiation hardness of any device based on graphene, and should be studied in detail [12].

The aim of the present work is to investigate the process of graphene perforation by SHI beams using atomic force microscopy (AFM) and Raman spectroscopy. This is accomplished by studying how the angle of irradiation influences the final size and shape of the nanopores. It is known that for grazing incidence SHI irradiation, 23 MeV I beam is needed for successful perforation of graphene [9]. However, the same SHI beam, leaves graphene intact when applied at normal incidence, although some degree of damage can be detected by Raman spectroscopy [13]. Thus, the role of the angle of irradiation in the perforation of graphene is still an unanswered question, as the minimal angle at which perforation of graphene occurs is unknown.

We hope to gain further insights by studying grazing incidence SHI irradiation of graphene at high fluences. Until now, grazing incidence SHI irradiation of graphene has been studied at low applied fluences, in order to avoid overlapping of ion tracks (permanent damage due to SHI impact via electronic stopping). Thus, graphene samples obtained in such experiments had low coverage of ion tracks, making them suitable for the AFM analysis. However, Raman spectroscopy studies

are still lacking because for the proper interpretation, high fluence datapoints are needed for the complete analysis using Lucchese model [7,14,15].

Finally, we aim to investigate the role that defects have on perforation of graphene. This will be achieved by pre-irradiating graphene with low energy ion beams, when damage can be induced in a controlled manner via nuclear stopping. In the next step, grazing incidence SHI irradiation will be applied and resulting nanostructures will be investigated both by AFM and Raman spectroscopy. At present, it is not known wether the presence of defects will promote perforation of graphene or not. Previous investigations of this type in other materials revealed both types of behavior. For example, in $SrTiO_3$ defects promote ion track formation [16], in graphite they play no role [17], while in SiC and Si the opposite is found, that defects can be erased by the SHI beams [18-21].

II. EXPERIMENTAL METHODS

The chemical vapor deposition (CVD) grown single-layer graphene samples were purchased from Graphenea, Spain. These graphene films were deposited on a 300 nm SiO_2/Si wafer as a substrate. Without any prior treatment, these samples have been irradiated by various ion beams. At Ruđer Bošković Institute, we used 6 MV Tandem Van de Graaff accelerator [22] for irradiation of samples at the ToF-ERDA beamline [23]. All of the used ion beams are listed in Table 1, with the ion beam irradiation parameters calculated using the SRIM code [24], under assumption that energy stopping of graphene and graphite are the same, and considering three graphene layers are 1 nm thick. Samples have been irradiated at various incidence angles. All irradiations have been done at room temperature and at the base pressure that has been kept below 10^{-6} mbar.

After irradiation, samples have been inspected by AFM and Raman spectroscopy. For the Raman spectroscopy measurements, we have used Horiba Jobin Yvon T64000 with a ×50 long working distance objective at Ruđer Bošković Institute. The green laser we used had an excitation wavelength of 532 nm and the power was kept under a few mW. To investigate the topography of the irradiated CVD-graphene, AFM measurements have been done using N'Tegra Prima (NT-MDT) microscope in the contact mode. In this way, it was possible to obtain surface topography images with a resolution of few nm. Obtained images were analyzed and reproduced by the Gwyddion code [25].

Table 1. List of swift heavy ion beams used in this work. Irradiation parameters were calculated for graphite using the SRIM code [24]

SHI	dE_e/dx (keV/nm)	dE_n/dx (keV/nm)	Range (μm)
1.8 MeV I	1.8	1.36	0.55
3 MeV Cu	2.05	0.25	1.70
10 MeV Cu	4.81	0.1	3.67
12 MeV Cu	5.38	0.09	4.06
18 MeV Cu	6.68	0.07	5.04
12 MeV Si	4.37	0.01	4.12

III. EXPERIMENTAL RESULTS AND DISCUSSION

When AFM measurements are done in the contact mode, there is an obvious contrast in the friction image between the graphene and the substrate surface due to different interactions between the AFM tip and respective surfaces, as illustrated in Fig.1. When the half transparent friction image is placed over topology (as shown in Fig.1b), both perforations in the graphene layer and folded graphene at the edges of perforations are more visible, while minor, relatively smooth variation in the height on graphene surface appear flatter. In all of the AFM images shown further down, the upper right quarter of image is replaced with this kind of display whenever the perforations occur.

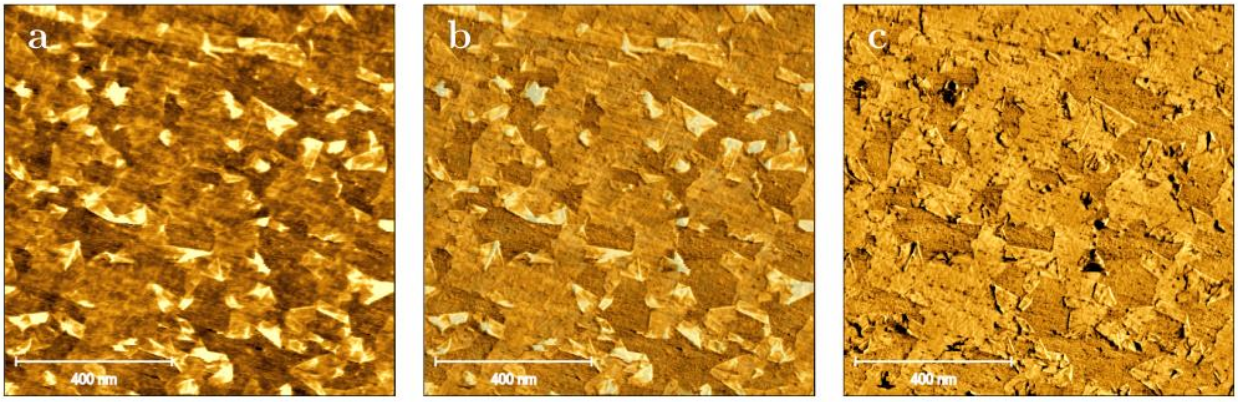

Figure 1. AFM images of 18 MeV Cu irradiated graphene at an angle $\alpha = 1.5°$, with the fluence $\Phi = 5\times10^{12}$ ions/cm^2, (a) topology, (c) friction and (b) half-transparent friction on top of topology.

Fig. 2 shows the results of AFM measurements on CVD-graphene irradiated with beams of different energies, where electron stopping is increasing gradualy from (a) to (f). In all cases, the angle of incidence α = 1.5° and fluence Φ = 5×10^{12} ions/cm^2 have been kept the same. Perforated graphene with foldings can be observed at higher values of electronic stopping (10 MeV Cu, 12 MeV Cu and 18 MeV Cu), while these are absent after irradiation by 3 MeV Cu and 12 MeV Si beams. Obtained threshold value for the perforation of graphene is therefore between S_e = 4.4 – 4.8 keV/nm, in good agreement with the previous result for the micromechanically exfoliated graphene [9]. However, we note that the applied ion fluence is quite large, and due to the small irradiation angle corresponds to ~1300 ion impacts per μm^2. Therefore, the observed nanostructures have evolved during irradiation, i.e. they have been generated by multiple SHI impacts. It appears that the 18 MeV Cu beam (the one that has the highest electronic stopping) is more efficient in generating such nanostructures than 12 or 10 MeV Cu beams, although in all cases large patches of graphene remained apparently unaltered.

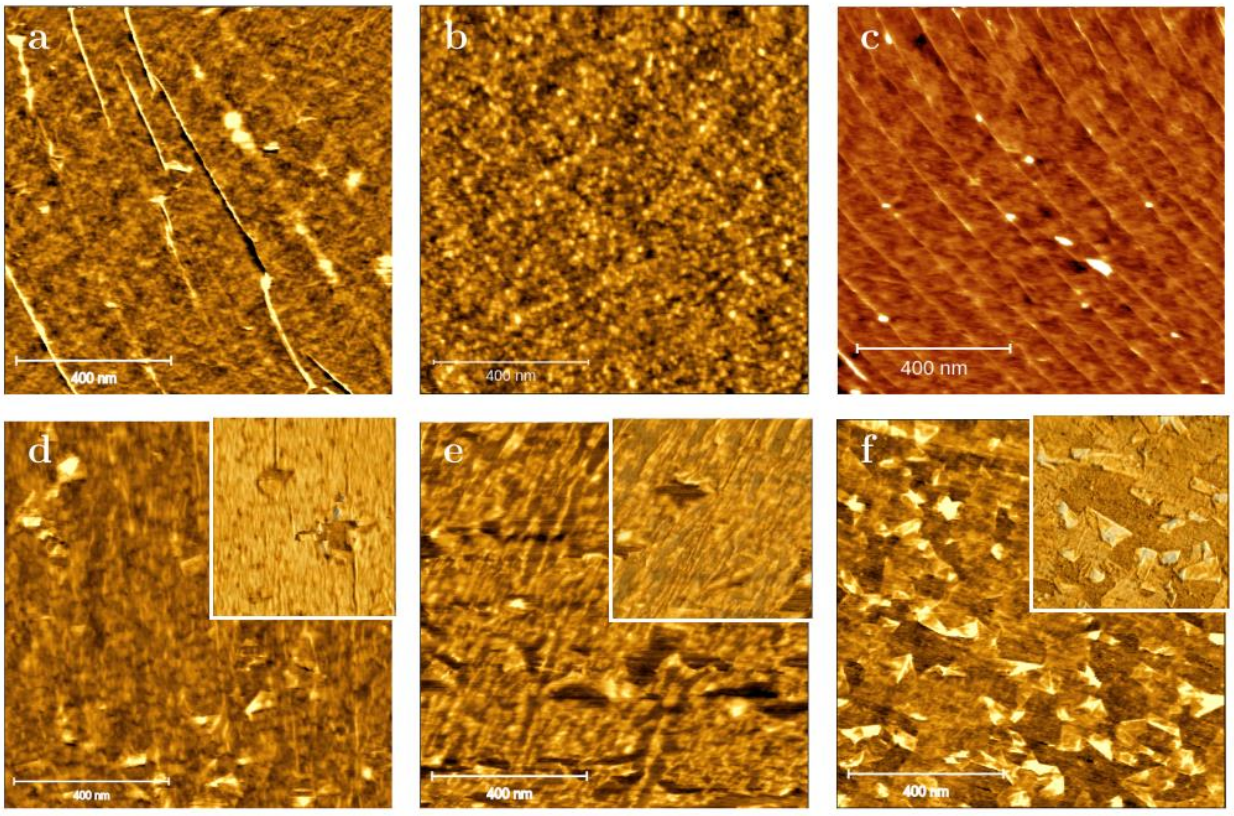

Figure 2. Graphene irradiated at an angle α = 1.5°, with the fluence Φ = 5×10^{12} ions/cm^2: (a) not irradiated, (b) 3 MeV Cu, (c) 12 MeV Si, (d) 10 MeV Cu, (e) 12 MeV Cu and (f) 18 MeV Cu.

Next, in Fig. 3 we show results of AFM measurements on CVD-graphene irradiated by 18 MeV Cu beam, when the fluence was kept constant (Φ = 5×10^{12} ions/cm^2), but the angle of irradiation was varied. It is clearly shown that with increasing angle, the nanostructure formation is less efficient, and already at angle α = 8° there are no apparent changes to the graphene sheet.

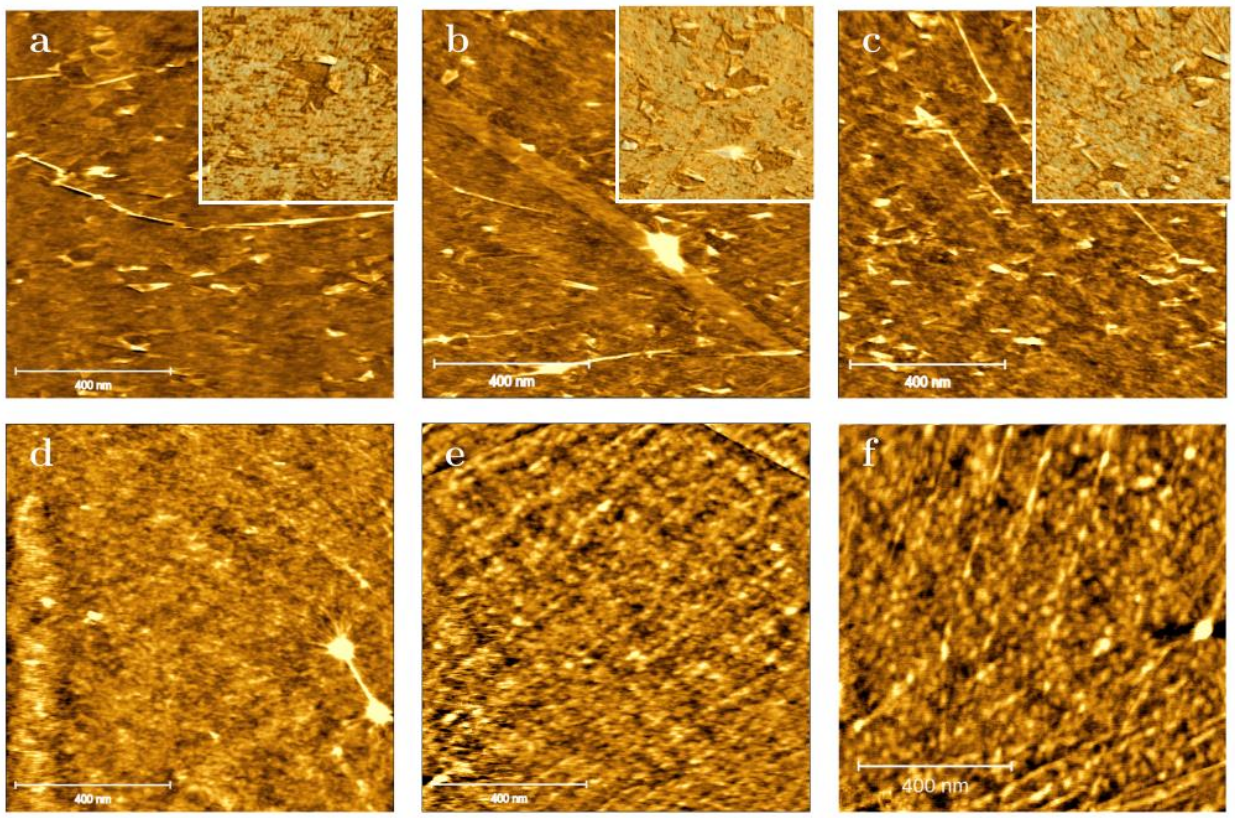

Figure 3. 18 MeV Cu irradiated graphene with the fluence Φ = 5×10^{12} ions/cm^2 at varying angles of incidence: (a) α = 0.5º, (b) α = 2º, (c) α = 4º, (d) α = 8º, (e) α = 15º and (f) α = 45º.

Fig. 4 shows how the nanostructuring of CVD-graphene evolves with the applied SHI fluence. In this case, we used an 18 MeV Cu beam, and all samples were irradiated at the same grazing incidence angle α = 1.5°. We found nanostructures after low SHI fluence (Φ = 1×10^{12} ions/cm^2) was applied, which corresponds to ~250 impacts per μm^2. However, such nanostructures were not observed on samples irradiated with even lower fluences (for example Φ = 4×10^{11} ions/cm^2, corresponding to ~100 impacts per μm^2). Although not every single ion impact produces an ion track when close to the ion track threshold [26,27], it is more likely that the observed

nanostructures are result of multiple ion impacts, as suggested by the observed incubation fluence [28]. SHI impacts initially weaken the graphene, by introducing vacancies and other point-like defects into its structure. This leads to fracturing and ultimately perforation of the graphene at a later stage, if suitable conditions are met. We also note that by increasing the SHI fluence, nanostructures evolve further, in a manner that resembles curling of graphene, leaving less and less unaltered graphene. It appears that this process ends at sufficiently high fluence, as not much difference is observed for graphene samples irradiated at highest fluences ($\Phi = 5\times10^{12}$ ions/cm^2 and $\Phi = 5\times10^{13}$ ions/cm^2).

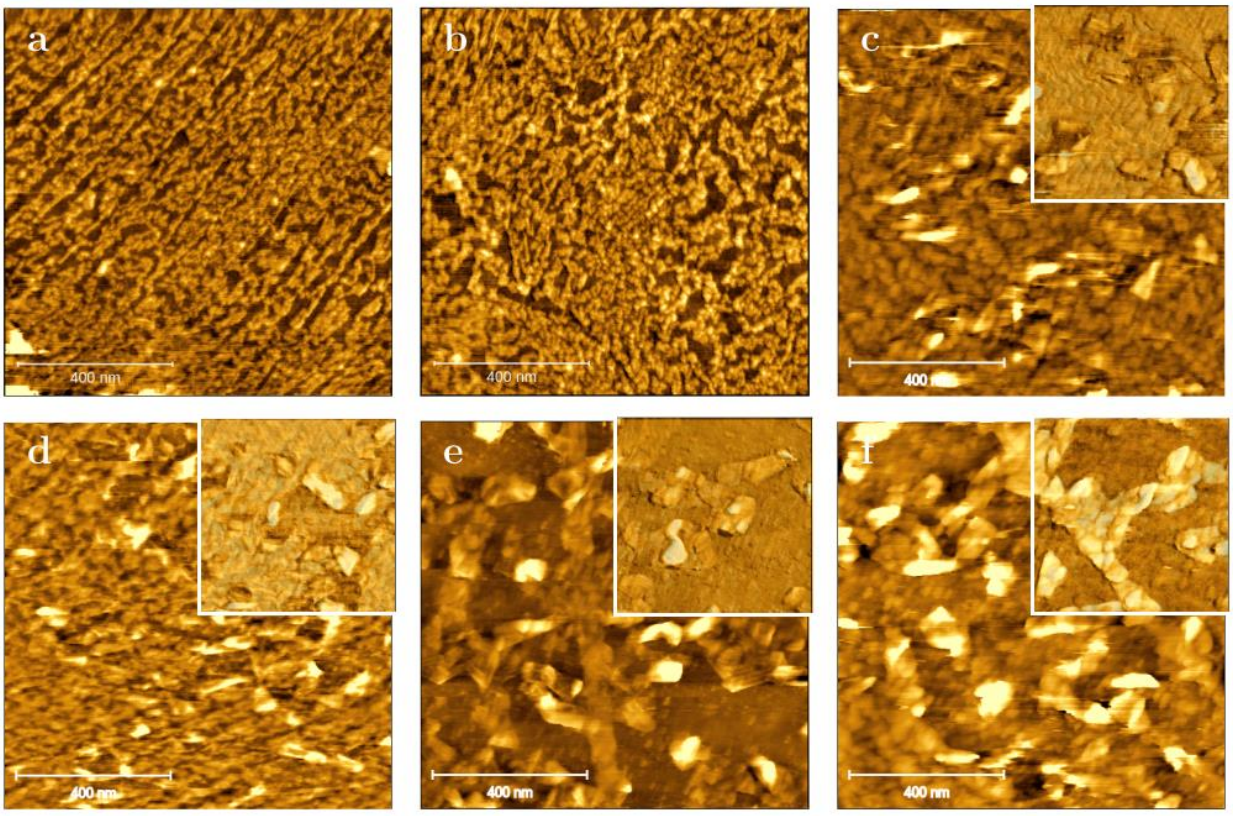

Figure 4. 18 MeV Cu irradiated graphene at an angle α = 1.5º with varying fluences: (a) $\Phi = 2\times10^{11}$ ions/cm^2, (b) $\Phi = 4\times10^{11}$ ions/cm^2, (c) $\Phi = 1\times10^{12}$ ions/cm^2, (d) $\Phi = 2\times10^{12}$ ions/cm^2, (e) $\Phi = 5\times10^{12}$ ions/cm^2, (f) $\Phi = 5\times10^{13}$ ions/cm^2.

Next, in Fig. 5 we present results of the AFM investigation on 12 MeV Si irradiated CVD-graphene. Besides the highest value of electronic stopping for which perforation does not occur, this beam (together with the 18 MeV Cu beam) has the lowest value of nuclear stopping, thus possible contribution from elastic collisions can be excluded. The observed ripples are not related

to the SHI irradiation, as they are result of the transfer process, and are also visible on the unirradiated sample. The 12 MeV Si beam is below the threshold for perforation of graphene, and therefore, all irradiated samples resemble unirradiated graphene. Nanostructures were not observed for any irradiation angle, nor for any applied fluence. Only for the highest fluence, the surface appears different, but this is most probably related to the response of the substrate to such a high fluence.

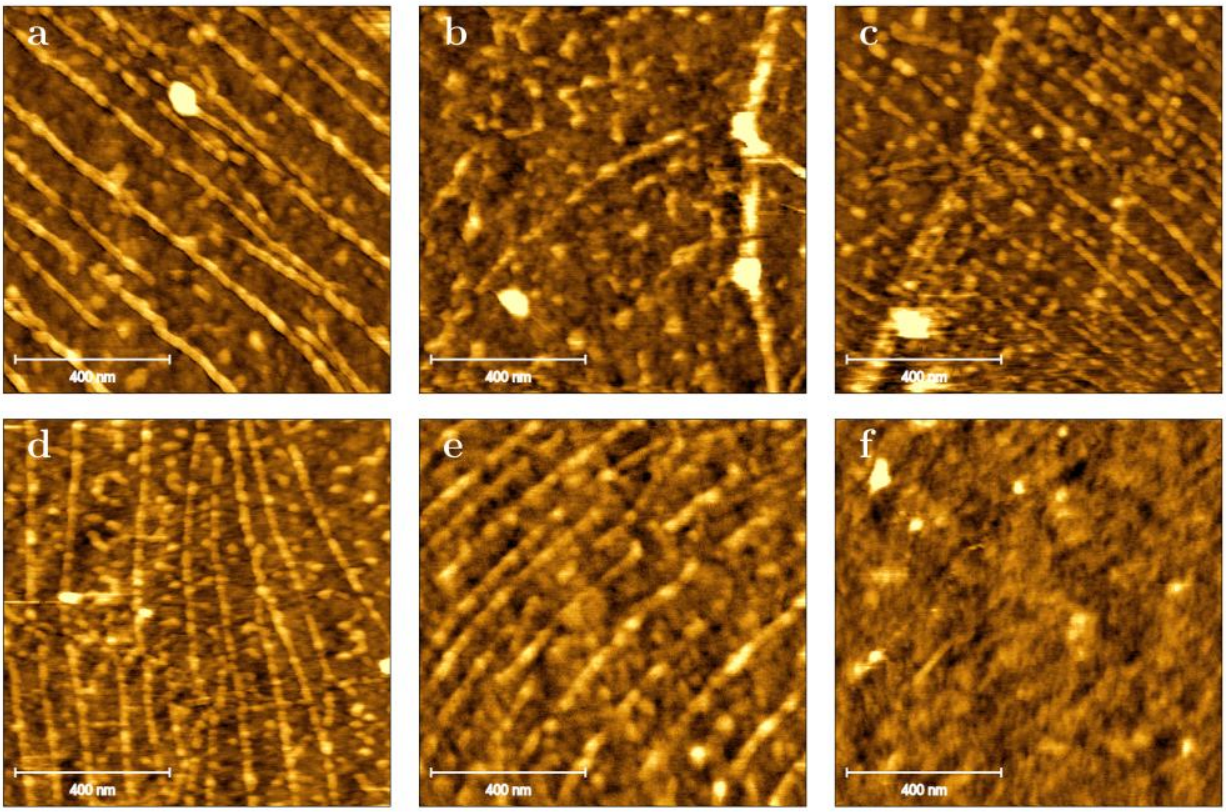

Figure 5. 12 MeV Si irradiated graphene, top row: fluence of 5×10^{12} ions/cm^2, at an angle (a) $\alpha = 0.5^{o}$, (b) $\alpha = 2^{o}$ and (c) $\alpha = 4^{o}$; bottom row: irradiated at an angle $\alpha = 1.5^{o}$ with the fluence: (d) $\Phi = 2\times10^{12}$ ions/cm^2, (e) $\Phi = 2\times10^{13}$ ions/cm^2 and (f) $\Phi = 2\times10^{14}$ ions/cm^2

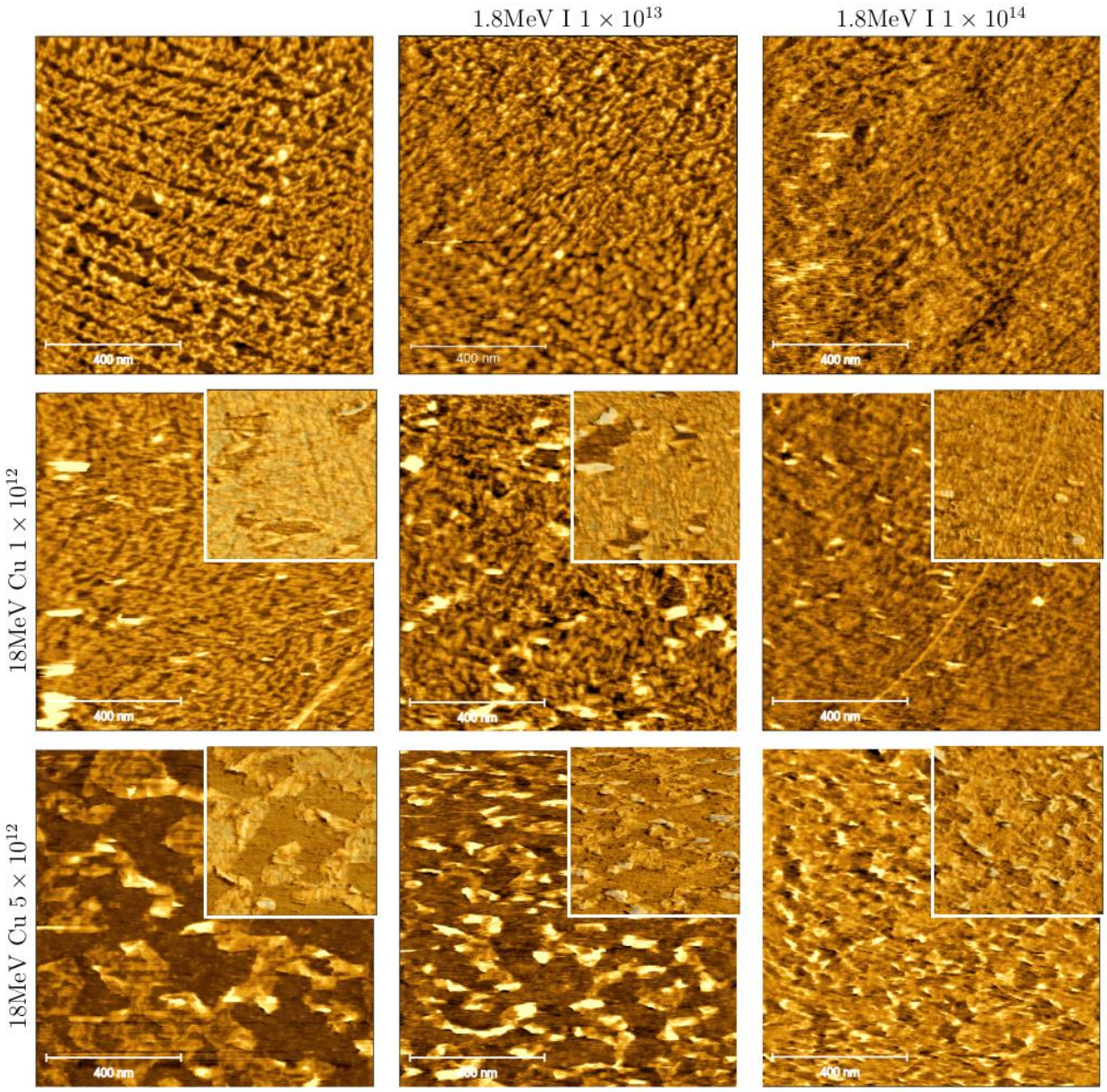

Figure 6. Sequentially irradiated graphene, first by normal ($\alpha = 90^o$) incidence 1.8 MeV I (middle column $\Phi_1 = 1\times10^{13}$ ions/cm^2 and right column $\Phi_1 = 1\times10^{14}$ ions/cm^2), then by grazing ($\alpha = 1.5^o$) incidence 18 MeV Cu (middle row $\Phi_2 = 1\times10^{12}$ ions/cm^2 and bottom row $\Phi_2 = 5\times10^{12}$ ions/cm^2). In the upper left corner is the image of the unirradiated graphene.

Finally, in Fig. 6, we present results of AFM investigations on sequentially irradiated CVD-graphene. In this case, graphene was initially irradiated with 1.8 MeV I at normal incidence, to the fluence of $\Phi_1 = 1\times10^{13}$ ions/cm^2 (middle column) or $\Phi_1 = 1\times10^{14}$ ions/cm^2 (right column). Then,

in the next step, these samples were irradiated by 18 MeV Cu beam at the grazing incidence angle $\alpha = 1.5°$, to the fluence of $\Phi_2 = 1\times10^{12}$ ions/cm^2 (middle row) or $\Phi_2 = 5\times10^{12}$ ions/cm^2 (bottom row). These results indicate that the damage introduced by the high fluence irradiation using 1.8 MeV I beam significantly affects the process of perforation and folding of graphene. The resulting nanostructures are smaller and there are only a few of them. On the other hand, pre-irradiation with 1.8 MeV I at low fluence doesn't lead to noticeable change in the response of graphene to 18 MeV Cu irradiation at grazing incidence. We also noticed that graphene irradiated only with 1.8 MeV I show no noticeable changes on the surface.

In the following, as shown in Fig. 7, we present spectra obtained by the Raman spectroscopy of irradiated graphene samples. We focused our attention to the samples irradiated by 18 MeV Cu (when perforation of graphene occurs) and 12 MeV Si (when perforation does not occur), so that we can correlate obtained AFM images with the measured Raman spectra. Additional Raman spectra from monolayer graphene irradiated by these same ion beams, but at normal incidence angle can be found in Ref. [29].

The primary information about the changes in the graphene due to SHI irradiation was obtained from the intensity ratio I_D/I_G of D (positioned around 1350 cm^{-1}) and G peak (positioned around 1580 cm^{-1}). According to the Lucchese model [7,14,15], amount of damage in the graphene is proportional to I_D/I_G until the damage due to individual SHI impacts starts to overlap at high fluences. Additional information can be obtained from the intensity ratio $I_D/I_{D'}$ of D and D' peak (positioned around 1620 cm^{-1}). When this ratio takes values above 10, it is usually assigned to sp^3-type defects, between 5 and 10 to vacancies, and below 5 to boundary-type defects [9,30]. Raman spectra shown in Fig. 7 have been analyzed (after background subtraction, all peaks have been fitted with the Lorentzian function) and the results are shown in Fig. 8, where intensity ratios I_D/I_G and $I_D/I_{D'}$ are shown as a function of the applied SHI fluence.

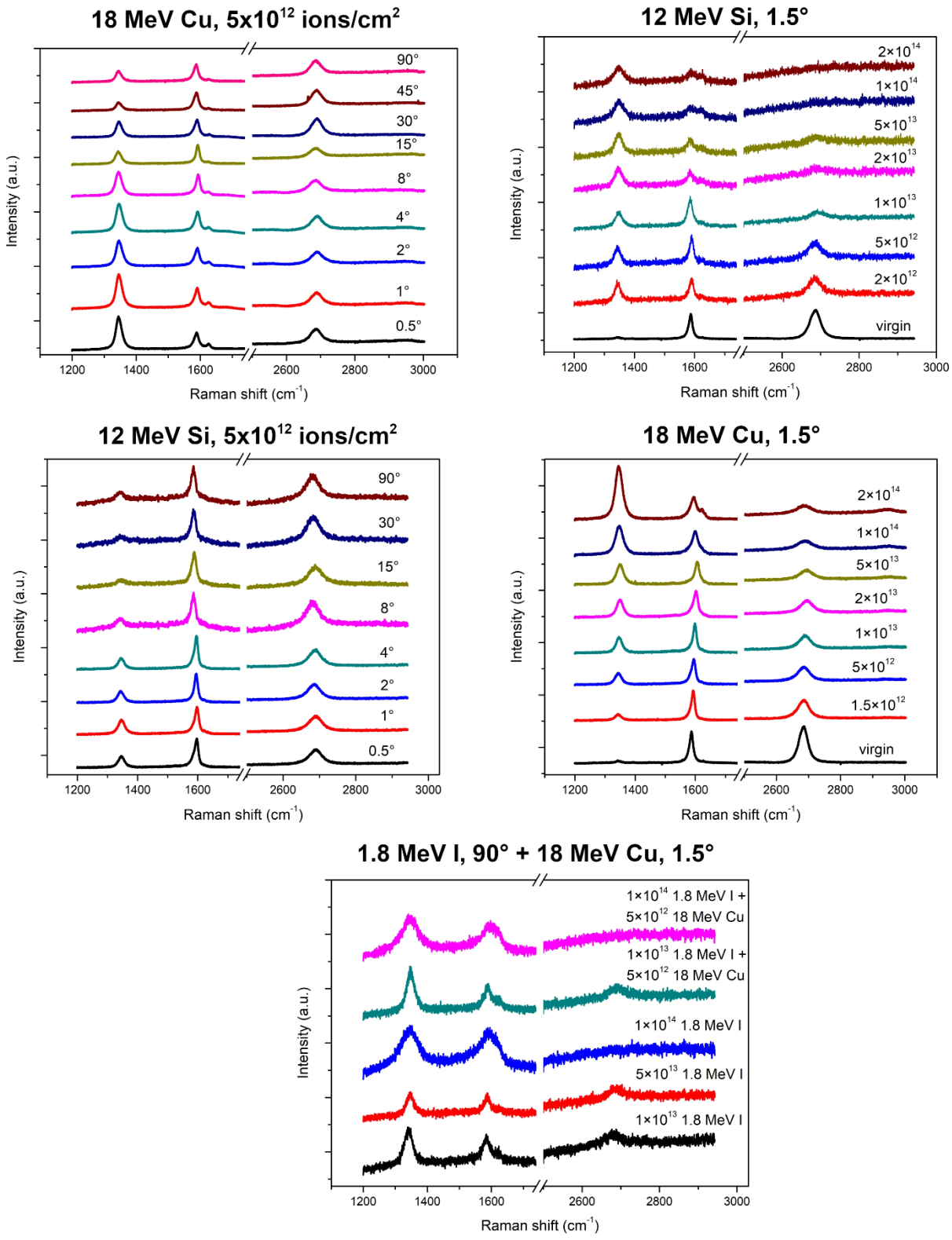

Figure 7. Raman spectra of graphene irradiated by 18 MeV Cu for (a) different angles and fixed fluence of $\Phi = 5\times10^{12}$ ions/cm^2 and (b) different fluences while keeping angle of irradiation fixed

at $\alpha = 1.5°$. Raman spectra of graphene irradiated by 12 MeV Si for (c) different angles and fixed fluence of $\Phi = 5\times10^{12}$ ions/cm^2 and (d) different fluences while keeping angle of irradiation fixed at $\alpha = 1.5°$. (e) Raman spectra obtained after 1.8 MeV I irradiation and after sequential irradiation with 1.8 MeV I at normal incidence ($\alpha = 90°$) and 18 MeV Cu ions at grazing incidence ($\alpha = 1.5°$).

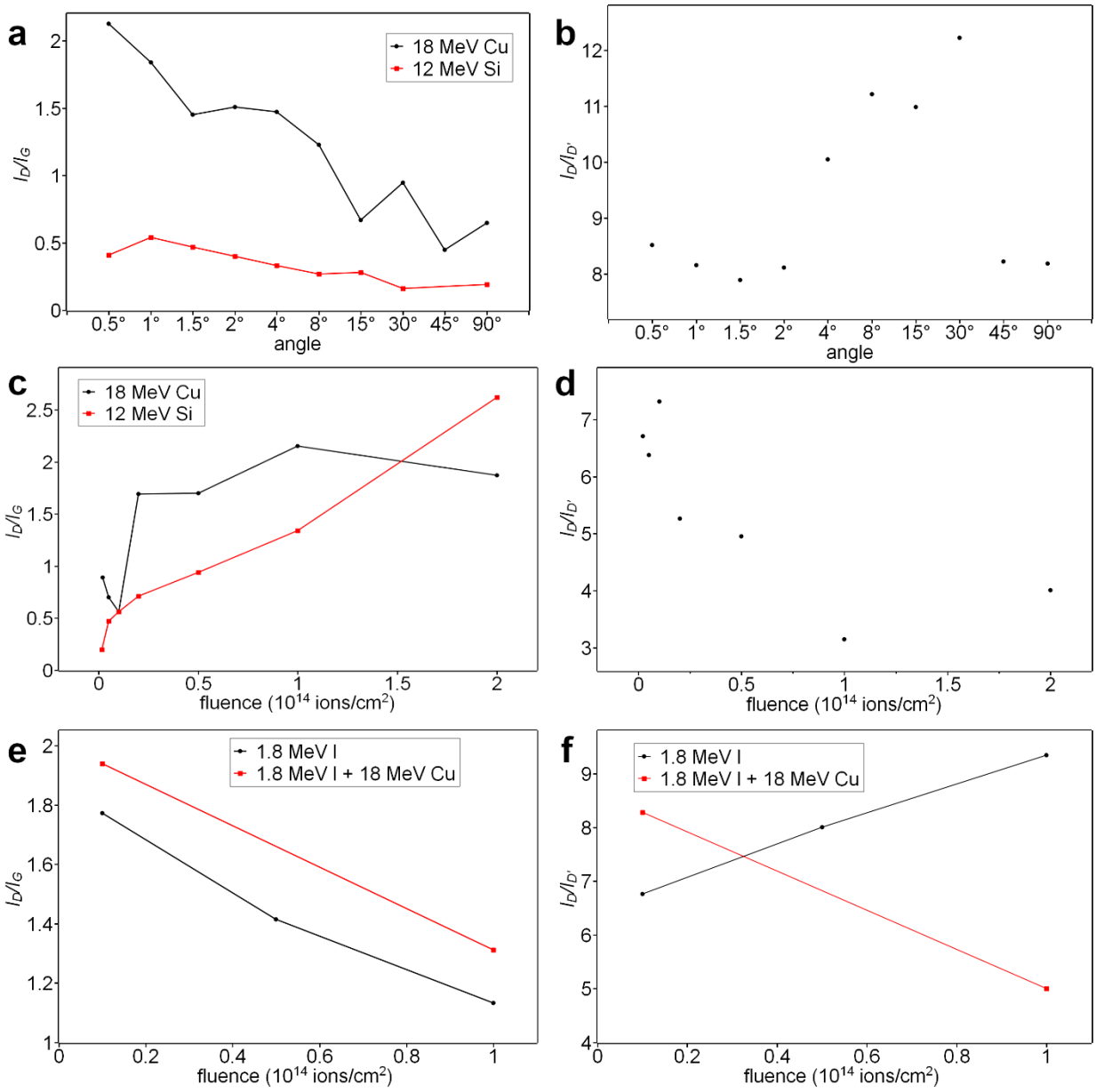

Figure 8. Peak intensity ratios (a) I_D/I_G and (b) $I_D/I_{D'}$ for Raman spectra obtained from graphene irradiated by 18 MeV Cu (black symbols) and 12 MeV Si (red symbols), for a fixed applied fluence

($\Phi = 5\times10^{12}$ cm^{-2}) and various angles of irradiation. Peak intensity ratios (c) I_D/I_G and (d) $I_D/I_{D'}$ for Raman spectra obtained from graphene irradiated by 18 MeV Cu (black symbols) and 12 MeV Si (red symbols), for a fixed angle of irradiation $\alpha = 1.5°$ and various fluences. Peak intensity ratios (e) I_D/I_G and (f) $I_D/I_{D'}$ for Raman spectra obtained from graphene irradiated by 1.8 MeV I (black symbols) and sequentially irradiated graphene (1.8 MeV I + 18 MeV Cu, red symbols), for various fluences of 1.8 MeV I. In case of sequential irradiations, applied ion fluence of 18 MeV Cu was 5×10^{12} ions/cm^2.

Fig. 8(a) shows the peak intensity ratio I_D/I_G as a function of angle of irradiation, both for 18 MeV Cu and 12 MeV Si beams. Since the applied fluence has been kept constant at $\Phi = 5\times10^{12}$ ions/cm^2, the larger I_D/I_G values for the 18 MeV Cu beam than for the 12 MeV Si indicate that the former beam is producing much more damage than the latter. This is consistent with the AFM data, as the 18 MeV Cu beam is able to perforate graphene, while 12 MeV Si cannot. The Raman data also suggest that graphene sustains a lot of damage by 18 MeV Cu beam at angles above $\alpha = 4^o$, even though perforation does not occur. Another feature of interest is related to the decrease of the I_D/I_G ratio when the angle of irradiation increases. Namely, grazing incidence SHI irradiation produces long surface ion tracks, whose length l can be related to the angle of irradiation via $l \sim 1/\tan(\alpha)$ [31]. On the other hand, the number of SHI impacts per unit surface area increases with the angle, proportionally to $\sin(\alpha)$. Therefore, the amount of damage, which is a product of the number of SHI impacts and the ion track length, should exhibit a cosine behavior, at least for small angles. However, the efficiency for damage formation as a function of angle is also a factor that should play a role, and could explain the highest levels of damage detected on samples irradiated by 18 MeV Cu at the smallest irradiation angles.

We also observe that the trend of decreasing I_D/I_G intensity ratio with increase of the angle of irradiation α is similar for both 18 MeV Cu and 12 MeV Si. Furthermore, this trend shows no discontinuity when perforation of graphene by 18 MeV Cu is no longer active at $\alpha = 8°$. For this reason, we analyzed the $I_D/I_{D'}$ ratio for 18 MeV Cu irradiated graphene, with intention to determine the type of defects which are predominant in perforated graphene. The results are shown in Fig. 8(b), and could be interpreted in the following manner. Under the irradiation conditions that lead to perforation of graphene, i.e. for 18 MeV Cu irradiations at incidence angles between $\alpha = 0.5°$ - 4°, vacancies are the majority of the defects produced. This is consistent with previous

observations that vacancies are required as a precursor for graphene perforation and folding [8,9]. For irradiations with 18 MeV Cu at higher angles (8° - 30°) when perforation of graphene doesn't occur, the $I_D/I_{D'}$ ratio indicates the presence of sp^3-defects. In case of 12 MeV Si irradiation, the D' peak is very small which again leads to the higher values of $I_D/I_{D'}$ ratio (data not shown in Fig. 8), resulting in the characteristic values for sp^3-defects. The only case in which $I_D/I_{D'}$ ratio indicates vacancies while perforation has not been observed was the case of very high irradiation angles (α = 45°, 90°) by 18 MeV Cu beam. In these cases, we consider it is possible that for sufficiently high applied fluence (in this case $\Phi = 5\times10^{12}$ ions/cm^2), the overlap of the ion impact areas occured, and consequently vacancies were formed. However, the low amount of energy deposited on the place of the SHI impact due to the large irradiation angle results in damage accumulation occuring without graphene perforation. A similar observation can be made in Fig. 8(d), when the overlapping of the 18 MeV Cu surface tracks at the highest fluences results in transformation of vacancies into boundary-type defects like dislocations. Again, the D' peak was found to be very small after 12 MeV Si irradiation, hence its $I_D/I_{D'}$ ratio was not plotted.

Raman spectroscopy of damage accumulation leading to perforation and folding of graphene, as shown in the AFM images presented in Fig. 4, indicates an incerasing I_D/I_G ratio with increasing fluence for the $\Phi = 10^{12}$ - 10^{14} ions/cm^2 range, as shown in Fig. 8(c). Only at the highest fluences I_D/I_G ratio reaches maximum, followed by a slight decrease. This indicates that the entire graphene surface has been affected by the 18 MeV Cu irradiation at a fluence of $\Phi = 5\times10^{13}$ ions/cm^2, when observed curling of the graphene has been finished. At present, further analysis similar to one used within Lucchese model is not possible due to the stretched morphology of the surface ion tracks (i.e. they are not round-shaped). Although irradiation with the 12 MeV Si beam at grazing incidence does not result in perforation of graphene (Fig. 5), it results in damage accumulation as shown by red symbols in Fig. 8(c). The accumulated damage which is predominantly sp^3-type, is also smaller than the damage produced by 18 MeV Cu because maximum I_D/I_G ratio has not been achieved even for highest 2×10^{14} ions/cm^2 fluence.

Finally, the results of the Raman spectroscopy of sequentially irradiated graphene are shown in Fig. 8(e,f) and the corresponding AFM images are shown in Fig. 6. Irradiation by 1.8 MeV I beam at normal incidence, introduces many defects in the impact areas that are heavily overlapping, which can be concluded from the decreasing I_D/I_G ratio in Fig. 8(e). Therefore, the slight increase of the I_D/I_G ratio after the exposure to 18 MeV Cu beam at grazing incidence

suggests damage recovery, but by a rather small amount. The $I_D/I_{D'}$ ratio shown in Fig. 8(f) indicates vacancy formation after 1.8 MeV I beam irradiation. Raman spectra obtained after subsequent irradiation by 18 MeV Cu show that defects of the same type are produced. Although, for the sample irradiated by the highest fluence of 1.8 MeV I, and subsequently by 5×10^{12} ions/cm^2 of 18 MeV Cu, transition from vacancies to the boundary-type of defects could be present. Such transformation might be needed to accommodate high damage levels, as the graphene's ability to reconstruct itself easily is well known [32]. In any case, absence of perforation and folding of graphene upon sequential irradiation at the highest doses indicates that both the density of defects and their type could play an important role in nanoscale perforation of graphene by SHI beams.

IV. CONCLUSION

In this work, we have investigated the perforation of CVD-graphene by grazing incidence swift heavy ion beams. By means of AFM, we have established threshold for the graphene perforation at 4.8 keV/nm (10 MeV Cu, irradiated at angle $\alpha = 1.5°$). However, the threshold also depends on the angle of irradiation, since 6.7 keV/nm (18 MeV Cu) was insufficient to perforate graphene when applied at the angle of $\alpha = 8°$. The perforation of graphene is most likely multi-ion impact process, which evolves with applied fluence, as curling of graphene was observed at high fluences. Raman spectroscopy indicated vacancies as a requirement for graphene perforation by swift heavy ions, in agreement with previous findings [9]. The role of defect density should be considered in the future, as pre-damaged graphene was found to be less susceptible to perforation.

Declaration of Competing Interest

The authors declare that they have no known competing financial interests or personal relationships that could have appeared to influence the work reported in this paper.

CRediT authorship contribution statement

P. Dubček: Conceptualization, Investigation, Formal analysis, Visualization, Validation, Writing – review & editing. **D. Iveković**: Conceptualization, Investigation, Formal analysis, Visualization,

Writing – review & editing. **T. Čižmar**: Investigation, Validation, Writing – review & editing. **M. Karlušić**: Conceptualization, Investigation, Validation, Supervision, Resources, Project administration, Funding acquisition, Writing – original draft.

Data availability

Data will be made available on request.

Acknowledgements

This work was supported by the Croatian Science Foundation (HrZZ project IP-2018-01-2786). D. I. acknowledges support by Croatian Science Foundation project "Young Researchers' Career Development Project – Training of Doctoral Students" funded by the European Union, Operational Program "efficient Human Resources 2014-2020" and the ESF. The financial support from the European Regional Development Fund for the 'Center of Excellence for Advanced Materials and Sensing Devices' (Grant No. KK.01.1.1.01.0001) is acknowledged.

REFERENCES

[1] Novoselov KS, Fal'ko VI, Colombo L, Gellert PR, Schwab MG, Kim K 2012 A roadmap for graphene *Nature* **192** 490

[2] Celebi K, Bucheim J, Wyss RM, Drouidan A, Gasser P, Shorubalko I, Kye J, Lee C, Park HG 2014 Ultimate Permeation Across Atomically Thin Porous Graphene *Science* **344** 289

[3] O'Hern SC, Boutilier MSH, Idrobo JC, Song Y, Kong J, Laoui T, Atieh M, Karnik R 2014 Selective Ionic Transport through Tunable Subnanometer Pores in Single-Layer Graphene Membranes *Nano Lett.* **14** 1234

[4] Madauβ L, Schumacher J, Ghosh M, Ochedowski O, Meyer J, Lebius H, Ban-d'Etat B, Tomil-Molares ME, Trautmann C, Lammertink RGH, Ulbricht M, Schleberger M 2017 Fabrication of nanoporous graphene-polymer composite membranes *Nanoscale* **9** 10487

[5] Vázquez H, Ahlgren EH, Ochedowski O, Leino AA, Mirzayev R, Kozubek R, Lebius H, Karlušić M, Jakšić M, Krasheninnikov AV, Kotakoski J, Schleberger M, Nordlund K, Djurabekova F 2017 Creating nanoporous graphene with swift heavy ions *Carbon* **114** 511

[6] Iveković D, Tomić Luketić K, Vázquez H, Leino AA, Djurabekova F, Nordlund K, Madauβ L, Liebsch Y, Schleberger M, Karlušić M 2024 Suspended nanoporous graphene produced by swift heavy ion bombardment *Mater. Chem. Phys.* **313** 128729

[7] Iveković D, Kumar S, Gajović A, Čižmar T, Karlušić M 2023 Response of Bilayer and Trilayer Graphene to High-Energy Heavy Ion Irradiation *Materials* **16** 1332

[8] Akcöltekin S, Bukowska H, Peters T, Osmani O, Monnet I, Alzaher I, Ban-d'Etat B, Lebius H, Schleberger M 2011 Unzipping and folding of graphene by swift heavy ions *Appl. Phys. Lett.* **98** 103103

[9] Ochedowski O, Lehtinen O, Kaiser U, Turchanin A, Ban-d`Etat B, Lebius H, Karlušić M, Jakšić M, Schleberger M 2015 Nanostructuring Graphene by Dense Electronic Excitation *Nanotechnology* **26** 465302

[10] Vázquez H, Kononov A, Kyritsakis A, Medvedev N, Schleife A, Djurabekova F 2021 Electron cascades and secondary electron emission in graphene under energetic ion irradiation *Phys. Rev. B* **103** 224306

[11] Iveković D, Žugec P, Karlušić M 2021 Energy Retention in Thin Graphite Targets after Energetic Ion Impact *Materials* **14** 6289

[12] Ochedowski O, Marinov K, Wilbs G, Keller G, Scheuschner N, Severin D, Bender M, Maultzsch J, Tegude FJ, Schleberger M 2013 Radiation hardness of graphene and MoS_2 field effect devices against swift heavy ion irradiation *J. Appl. Phys.* **113** 214306

[13] Tomić Luketić K, Hanžek J, Mihalcea CG, Dubček P, Gajović A, Siketić Z, Jakšić M, Ghica C, Karlušić M 2022 Charge State Effects in Swift-Heavy-Ion-Irradiated Nanomaterials *Crystals* **12** 865

[14] Lucchese MM, Stavale F, Martins Fereira EH, Vilani C, Moutinho MVO, Capaz RB, Achete CA, Jorio A 2010 Quantifying ion-induced defects and Raman relaxation length in graphene *Carbon* **48** 1592

[15] Zeng J, Liu J, Yao HJ, Zhai PF, Zhang SX, Guo H, Hu PP, Duan JL, Mo D, Hou MD, Sun YM 2016 Comparative study of irradiation effects in graphite and graphene *Carbon* **100** 16

[16] Weber WJ, Zarkadoula E, Pakarinen OH, Sachan R, Chisholm MF, Liu P, Xue H, Jin K, Zhang Y 2015 Synergy of elastic and inelastic energy loss on ion track formation in $SrTiO_3$ *Sci. Rep.* **5** 7726

[17] Iveković D, Dubček P, Gajović A, Čižmar T, Radatović B, Brkić AL, Kralj M, Karlušić M 2023 High-energy heavy ion irradiation of HOPG *J. Nucl. Mater.* **578** 154370

[18] Benyagoub A, Audren A, Thomé L, Garrido F 2006 Athermal crystallization induced by electronic excitations in ion-irradiated silicon carbide *Appl. Phys. Lett.* **89** 241914

[19] Zhang Y, Sachan R, Pakkarinen OH, Chisholm MF, Liu P, Xue H, Weber WJ 2015 Ionization-induced annealing of pre-existing defects in silicon carbide *Nature Commun.* **6** 8049

[20] Hanžek J, Fazinić S, Kumar S, Karlušić M 2024 Threshold for ionization-induced defect annealing in silicon carbide *Radiat. Phys. Chem.* **215** 111362

[21] Tomić Luketić K, Karlušić M, Gajović A, Fazinić S, O'Connell JH, Pielić B, Radatović B, Kralj M 2021 Investigation of Ion Irradiation Effects in Silicon and Graphite Produced by 23 MeV I Beam *Materials* **14** 1904

[22] Jakšić M, Bogdanović Radović I, Bogovac M, Desnica V, Fazinić S, Karlušić M, Medunić Z, Muto H, Pastuović Ž, Siketić Z, Skukan N, Tadić T 2007 New capabilities of the Zagreb ion microbeam system *Nucl. Instr. Meth. Phys. Res. B* **260** 114

[23] Siketić Z, Bogdanović-Radović I, Jakšić M 2008 Development of a time-of-flight spectrometer at the RuđerBošković Institute in Zagreb *Nucl. Instr. Meth. Phys. Res. B* **266** 1328

[24] Ziegler JF, Ziegler MD, Biersack JP 2010 SRIM – the stopping and range of ions in the matter (2010) *Nucl. Instr. Meth. Phys. Res. B* **268** 1818

[25] Nečas D, Klapetek P 2012 Gwyddion: an open-source software for SPM data analysis *Cent. Eur. J. Phys.* **10** 181

[26] Khalfaoui N, Rotaru CC, Bouffard S, Toulemonde M, Stoquert JP, Haas F, Trautmann C, Jensen J, Dunlop A 2005 Characterization of swift heavy ion tracks in CaF_2 by scanning force and transmission electron microscopy *Nucl. Instrum. Meth. Phys. Res. B* **240** 819

[27] Kaur R, Ström P, Primetzhofer D 2023 Surface characterization of CaF_2 crystals irradiated with MeV ions below charge state equilibrium *Nucl. Instrum. Meth. Phys. Res. B* **536** 132

[28] García G, Rivera A, Crespillo ML, Gordillo N, Olivares J, Agulló-López F 2011 Amorphization kinetics under swift heavy ion irradiation: A cumulative overlapping-track approach *Nucl. Instrum. Meth. Phys. Res. B* **269** 492

[29] Tomić Luketić K, Gajović A, Karlušić M 2024 High-energy heavy ions as a tool for production of nanoporous graphene *Appl. Surf. Sci.* **669** 160593

[30] Eckmann A., Felten A, Mishchenko A, Britnell L, Krupke R, Novoselov KS, Casiraghi C 2012 Probing the Nature of Defects in Graphene by Raman Spectroscopy *Nano Lett.* **12** 3925

[31] Akcöltekin E, Akcöltekin S, Osmani O, Duvenbeck A, Lebius H, Schleberger M 2008 Swift heavy ion irradiation of $SrTiO_3$ under grazing incidence *New J. Phys.* **10** 053007

[32] Zan R, Ramasse QM, Bangert U, Novoselov KS 2012 Graphene Reknits its holes *Nano Lett.* **12** 3936